Available online at www.sciencedirect.com

ScienceDirect

Procedia Engineering 4 (2010) 311–318

Procedia Engineering

www.elsevier.com/locate/procedia

ISAB-2010

Modeling of Qiandao Lake submerged floating tunnel subject to multi-support seismic input

Luca Martinelli[a]*, Gianluca Barbella[a], Anna Feriani[b]

[a]*Department of Structural Engineering, Politecnico di Milano, Piazza Leonardo da Vinci 32, 20133 Milan, Italy*
[b]*D.I.C.A.T.A., University of Brescia, via Branze 43, 25123 Brescia, Italy.*

Received 14 July 2010; revised 29 July 2010; accepted 30 July 2010

Abstract

The modeling and seismic analysis of Qiandao lake submerged floating tunnel (SFT) is addressed with particular attention to the mooring system, to dissipation issues and to the spatial variability of the excitation, within a numerical procedure developed by the research group to perform the step-by-step dynamic analysis of discretized non-linear structural systems. The procedure, which can handle arbitrary external loading allowing for multiple-support seismic excitation, is enhanced by enriching the mooring cables model adding non-linear hydrodynamic loads. Different dissipation models account for hydrodynamic damping, structural damping and radiation damping which are included, respectively, as non-linear forces, as linear viscous damping equivalent to linear hysteretic by means of an iterative procedure, and as linear viscous damping. A possible solution is here studied to define an adequate cable discretization in order to correctly model nonlinear geometric effects and to avoid fictitious compressions. A uniformly modulated random process, whose spatial variability is governed by a single coherency function, is deemed adequate to model multi-support seismic input for the given structure. A novel method to obtain response spectrum compatible accelerograms is here proposed.

Keywords: nonlinear dynamics; geometric effects; multi-support seismic excitation

1. Introduction

Earthquakes induce not only inertial loads but also hydrodynamic ones. The modeling of the latter is non-linear, as is the response of the anchoring cables, whose geometrically non-linear behaviour depends on the SFT buoyancy effect. The spatial variability of the ground motion must be considered if the SFT length requires it.

The mooring cables model is included in the numerical procedure developed by the research group to perform the step-by-step dynamic analysis of discretized non-linear structural systems under arbitrary external loading, allowing for multiple-support seismic excitation. A Lagrangian three-node isoparametric cable element formulated in the small-strain large-displacement hypothesis is adopted, whose element matrices and internal forces vector are directly

* Corresponding author. Tel.: +39-(0)2-23994247; fax: +39-(0)2-23994220.
E-mail address: luca.martinelli@polimi.it

1877-7058
doi:10.1016/j.proeng.2010.08.035

computed in the global coordinates system, so that the assembling procedure needs no transformation. In order to model submerged cables, the added mass matrix and the non-linear hydrodynamic loads were implemented. Morison approach was adopted. In order to correctly model nonlinear geometric effects and to avoid fictitious compressions, an adequate cable discretization is sought; simplified analyses proved adequate to choose a number of elements that guarantees the absence of compressions being however efficient.

Hydrodynamic damping forces are modeled as non-linear, while a linear damping matrix accounts for the hysteretic damping of the SFT subsystems (tunnel, cables and foundations). Soil radiation damping is accounted for separately. The modeling of structural damping is improved by merging two previous procedures, obtaining a banded damping matrix referred to the static configuration, which respects the global modal damping ratios of the combined system.

A uniformly modulated random process is deemed adequate to model seismic input for the given structure. A novel method to obtain response spectrum compatible accelerograms is proposed, that is based on the explicit expression of the median pseudo-acceleration Response Spectrum (RSa) of the spectral power density function (PSD) selected for the seismic input. The RSa is then used to identify the parameters of the PSD function that minimize the difference with the elastic response spectrum prescribed by EN 1998 [1]. Samples of the free-field motion are subsequently generated using a proved and theoretically sound approach, reaching a satisfactory agreement with the prescribed response spectra. The seismic response of the SFT is discussed.

2. The cable element

The three-node isoparametric Lagrangian cable element is derived from the explicit formulation proposed in [2] with reference to the static case, extended to the dynamic case and coded in [3] to fully consider the non-linear effects of the motion of the structure on aerodynamic interaction forces. The single element matrices and internal forces vectors are directly computed with respect to the global coordinates system, so that no transformation is needed in the assembling procedure. In the numerical implementation of the element, the elemental mass matrix and the elastic stiffness terms have been evaluated in closed form, while two points Gauss quadrature has been used for the geometric stiffness and for internal forces.

2.1. Hydrodynamic loading

The relative velocity model within the framework of the Morison-Chakrabarti [4] approach, which is well justified, from geometrical considerations for the anchor cables, is adopted, neglecting tangential forces. Accordingly, the wave force per unit length acting on a moving cylinder is a function of the components of relative velocity $(\boldsymbol{w}-\dot{\boldsymbol{u}})$, water acceleration $\dot{\boldsymbol{w}}$, and element acceleration $\ddot{\boldsymbol{u}}$, normal to the element axis, i.e.:

$$\boldsymbol{f}=\frac{1}{2}C_D\rho D\left|\boldsymbol{w}_\perp-\dot{\boldsymbol{u}}_\perp\right|\left(\boldsymbol{w}_\perp-\dot{\boldsymbol{u}}_\perp\right)+C_M\rho\frac{\pi}{4}D^2\dot{\boldsymbol{w}}_\perp-C_A\rho\frac{\pi}{4}D^2\ddot{\boldsymbol{u}}_\perp \tag{1}$$

where the subscript $\perp$ denotes the orthogonal components with respect to the element axis, ρ, D, C_D, C_M are the fluid density and the element diameter, drag and inertia coefficients and $C_A=C_M-1$ is the added mass coefficient. The first term on the right hand side of Eq. (1) represents the drag loading, the second the inertia loading, the third the added mass effect. The first two contributions of Eq. (1) have been dealt with as distributed loads, evaluated exactly at the nodes, and interpolated parabolically along the element; a two points Gauss quadrature determines the vector of the equivalent nonlinear dynamic nodal forces. The last term, depending on the element accelerations, yields to the determination of the added mass contribution. Considering only the last term in Eq. (1), and integrating over the length L, we obtain

$$\boldsymbol{R}_{Madd}=-C_A\rho\frac{\pi}{4}D^2\int_0^L\boldsymbol{H}^T\ddot{\boldsymbol{u}}_\perp\,\mathrm{d}s \tag{2}$$

where $\mathbf{H}(s)$ is the shape functions matrix, s being the intrinsic curvilinear coordinate, ranging from 0 to L, the length of the element. The normal components of the element acceleration vector can be expressed as:

$$\ddot{\boldsymbol{u}}_{\perp}(s) = \boldsymbol{\alpha}(s)\ddot{\boldsymbol{u}}(s) = \boldsymbol{\alpha}(s)\boldsymbol{H}(s)\ddot{\boldsymbol{u}} \tag{3}$$

where the transform matrix $\boldsymbol{\alpha}(s)$ is related to the direction cosines of the tangent to the cable axis. Finally, integrating at the Gauss points, the local added mass contribution is given by:

$$\boldsymbol{M}_{add} = k_M \sum_{k=1}^{2} w_k \left[\boldsymbol{H}^T \boldsymbol{\alpha} \boldsymbol{H}\right]_{s_k} \text{ with } k_M = C_A \rho \frac{\pi}{4} D^2 \tag{4}$$

where w_k is the weight of the k^{th} quadrature point s_k. It is important to notice that matrix $\boldsymbol{\alpha}(s)$ strongly depends on the current system configuration. So do the orthogonal component of water velocity, water acceleration, element acceleration, and consequently both the hydrodynamic forces and the added mass matrix. These quantities are updated at the end of each time step.

2.2. Discretization issues

The geometrical constraint represented by the isoparametric approximation does not allow the numerical model to correctly reproduce the natural cable behaviour, which modifies its shape so that only tractions occur. If the discretization is not adequate the final shape cannot be modelled and fictitious compressions can arise, which must be avoided.

In order to reach an efficient but adequate discretization of the tethers, in [5], with reference to a different SFT, a plane model of a section of the tunnel was considered. Cables response to seismic excitation was analyzed varying the discretization degree. The single tether was modeled with 1, 2, 5 or 10 elements. Five elements per tether emerged as the best compromise between accuracy and computational cost in the light of the complete model, since no significant differences could be noted using more elements. In the present work, this same refinement level was adopted in order to model correctly the cables buckling while limiting the number of DOFs; its adequateness was proved by the results described in [6].

3. Dissipation effects

Since dissipation effects due to the non-linear hydrodynamic forces are accounted for at the r.h.s. of the equations of motion, the damping matrix **C** at the l.h.s. accounts for the ground radiation damping and for the soil-structure hysteretic damping, which is not uniform due to the presence of different subsystems (for instance, for the SFT considered in this work, soil, cables, end-restraints, tunnel).

According to the results of the comparisons presented in [7], frequency response functions relative to significant response parameters such as internal actions are well approximated if the damping matrix is built following the procedure called CSMD (Combined System Modal Damping) therein. The CSMD procedure consists in (1) applying the “weighted damping” method [8] to the system components characterized by hysteretic damping, obtaining modal damping ratios; (2) building the corresponding viscous matrix, which is full; (3) directly adding viscous elements which, if a lumped parameter approach is adopted, model radiation damping.

Such procedure is here modified with respect to steps 1 and 2. First, since a non-linear dynamic analysis is to be performed, in steps 1 and 2 a tunnel model linearized with respect to the static equilibrium configuration is considered. Then, in order to reduce computation times, before moving to step 3, the equivalent viscous damping matrix obtained at step 2 is modified according to the iterative procedure described in [9], obtaining a reduced bandwidth matrix while retaining, within a given tolerance, the assigned modal damping ratios.

4. Generation of the seismic ground motion

The method by Monti et al. described in [10], which relies on the proven spectral representation method by Shinozuka [11], is adopted to generate acceleration time histories which satisfy the same PSD function at all stations and have cross-PSD functions depending on one coherency function only. In the present work, as an innovation, the parameters of the PSD are carefully chosen according to the procedure described in [6] in order to minimize the difference between the consequent pseudoacceleration response spectrum RS_a and the one prescribed by Eurocodes $S_{e,,EN1998}$.

The coherency function is that proposed by Luco and Wong [12], disregarding local effects :

$$\gamma\left(\xi,\omega\right)=e^{-\left(\frac{\alpha\omega\xi}{v_S}\right)^2}e^{i\frac{\omega\xi_L}{v_{app}}} \tag{5}$$

in Eq. (5) the modulus decays exponentially with the horizontal distance ξ between the stations, with the circular frequency ω, and inversely with the mechanical properties of the ground condensed by the ratio vs/α. The phase depends linearly on ω, on the relative distance ξL and on the inverse of the apparent velocity at the surface, vapp, of the seismic perturbation. In the generation process, the phase given by the imaginary part in Eq. (5) leads to a time delay only, which is due to the finite wave propagation velocity.

The direct PSD Sii of the underlying process, here adopted, is the Clough and Penzien PSD [13], which can be viewed as the effect of a filter, representing the soil, on a white noise process of intensity S0 which represents, in turn, the motion of the bedrock:

$$S_g\left(\omega\right)=S_0S_{CP}\left(\omega\right)\;=\;S_0\frac{\omega_1^4+4\xi_1^2\omega_1^2\omega^2}{\left(\omega_1^2-\omega^2\right)^2+4\xi_1^2\omega_1^2\omega^2}\frac{\omega^4}{\left(\omega_2^2-\omega^2\right)^2+4\xi_2^2\omega_2^2\omega^2} \tag{6}$$

ω_1 and ξ_1 are the parameters of the Kanai-Tajimi filter representing the soil natural frequency and damping ratio, respectively, while ω_2 and ξ_2 are the parameters of an additional high-pass filter introduced by Clough and Penzien to guarantee that displacements possess finite power. However, such parameters are chosen in order to satisfy the minimization process described in [6], which takes advantage of the explicit expression of the RS_a consequent to (6), given therein for the first time, to the Authors' knowledge.

The underlying stationary process $x(t)$ generated in such way is then uniformly modulated multiplying it by a deterministic envelope $f(t)$:

$$\begin{aligned} f &= (t/t_0)^2 && 0<t<t_0 \\ f &= 1.0 && t_0<t<t_n \\ f &= e^{-0.155(t-t_n)} && t_n<t \end{aligned} \tag{7}$$

In this work, the parameters of the PSD have been chosen so that RS_a complies with the "type 1" EN 1998 elastic design spectra for a type "C" soil. Two sets of parameters, for the explicit expression of RS_a obtained in [6], have been identified by minimizing the error with the elastic design spectra S_e and S_{ve} respectively. A damping ratio ξ_s =0.05 was considered in the fittings since the EN 1998 spectra refer to such damping. Another parameter that influences RS_a is the process duration s_0 , which is taken equal to the strong motion duration, $t_{max}= t_n–t_0$ =10s. The minimization process was carried out with respect to the period range T_i=0.001-T_u=2s. The identified values of ω_1, ξ_1, ω_2, ξ_2, S_0 are listed in Table 1. The visual comparison with the target spectra is depicted in Fig. 1(a) and 1(b).

Table 1. Values of the parameters that minimize the error with the "type 1" EN 1998 horizontal (S_e) and vertical (S_{ve}) elastic design response spectrum in the periods range 0.001-2s for type "C" soil

Component	ω_1 (rad s^{-1})	ζ_1	ω_2 (rad s^{-1})	ζ_2	S_0 (m^2 $s^{-4}Hz^{-1}$)
S_e	12.02	0.6926	0.3180	3.971	0.001953
S_{ve}	53.95	0.6338	3.50	1.22	$3.382x10^{-4}$

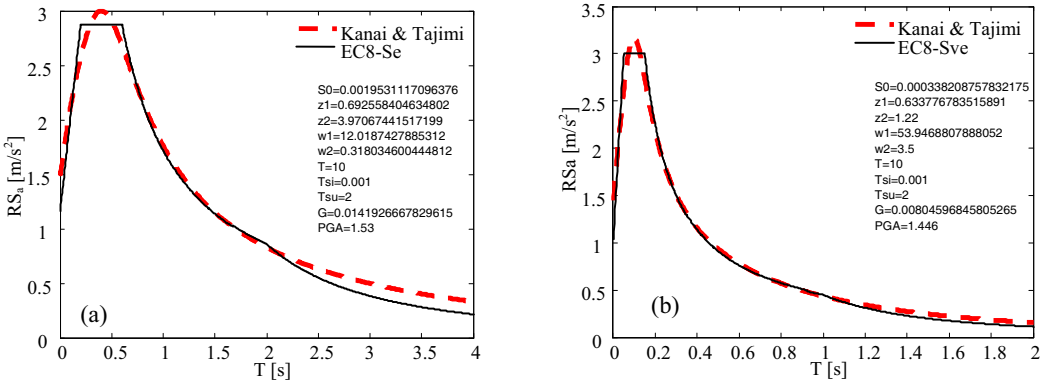

(a) (b)

Fig. 1. Comparison of target pseudo-acceleration spectrum with EN 1998 elastic design one, for (a) Horizontal; (b) Vertical components of ground motion

5. Seismic analysis of the Qiandao lake SFT model

Seismic analyses consider the SFT model [14] making reference to the bed profile of Qiandao Lake. The maximum water depth is about 30 m, while the total length of the crossing is 100 m. The tunnel axis is placed 9.2 m below the still water level.

5.1. The tunnel structure

The tunnel is divided into five 20 m long modules having a composite cross-section composed of an internal steel cylinder, 20 mm thick, a middle reinforced concrete (RC) layer, 300 mm thick, and a protective aluminum coating, 100 mm thick. The joint between adjacent modules assures the bending resistance of the composite cross-section while provides that of only the steel section in tension. The tunnel dead weight is equal to 115 kNm^{-1}, the maximum live load to 10 kNm^{-1}, whereas the Archimedes buoyancy is 160 kNm^{-1}. A non-linear dissipation device working in the longitudinal direction is introduced at one end, the yielding force being set to one tenth of the tunnel weight, while at the other end of the tunnel the axial motion is left free. The anchoring to the lake bed is guaranteed by three cables systems (see Fig. 2): at the center of the second, third and fourth module, respectively. The ropes nominal diameter is 40 mm for the second and fourth modules, and 60 mm for the central one, with an effective axial area of 1090 mm^2 and 2490 mm^2 respectively. The equivalent Young modulus is 140000 MPa. Gravity type block foundations are considered for each group of anchoring cables.

The tunnel is modeled by means of 6 elastic 3D beam elements for each module; the beam properties refer to the composite section considering perfect bond between steel and RC.

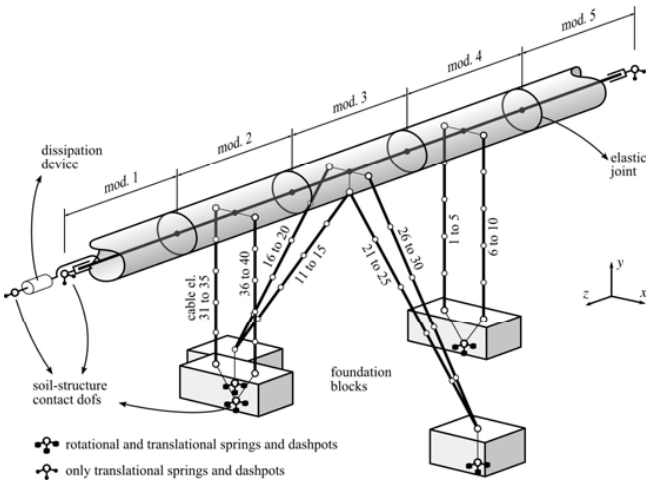

Fig. 2. Scheme of the tunnel model

The modules joints are modeled considering only the steel section in evaluating the beam stiffness. The resisting cross-section mechanical and geometric characteristics, homogenized to steel, are listed in Table 2:

Table 2. Tunnel cross-section mechanical and geometric characteristics.

Young Modulus (MPa)	Area (m^2)	Shear Area (m^2)	Inertia (m^4)
206000	0.748	0.374	1.354

Cable elements have distributed masses while those of the tunnel are lumped at nodes; as for the tunnel, the added mass effect is considered in both vertical and transverse directions.

At both tunnel ends flexural and twist rotations are free, while an elastic connection to the foundation is assumed for vertical and transverse translations. In the axial direction, the dissipative device installed at one of the ends (herein, at z = 100 m) is modeled using an elastic-plastic spring with kinematic hardening, the initial stiffness being set to provide a natural period of 1 s for the longitudinal rigid-body motion of the tunnel.

Anchorings are discretized with the three-node isoparametric cable element recalled in Section 2. Each cable is divided into 5 elements, since preliminary comparisons summarized in Section 2.2 showed that such discretization is generally adequate in avoiding fictitious compressions. The connection between the beams modeling the tunnel and the cables end nodes is imposed with rigid link elements, so that torsional effects are considered. Soil-structure interaction is taken into account by assuming a lumped-parameters approach. Thus six springs, placed at the centroid of the foundation-ground interface, model the soil translational and rotational stiffness, while six linear dashpots, acting in parallel to the springs, account for elastic wave radiation. The springs and dashpots approximate the impedance of a homogeneous half-space [15], having a shear modulus equal to 100000 kPa, a Poisson coefficient of 0.33 and a mass density equal to 2 tm^{-3}. It is assumed that the abutments have dimensions similar to those of the foundation blocks.

The damping matrix equivalent to the hysteretic effects of elastic elements is assembled according to the procedure outlined in Section 3. Different hysteretic damping ratios have been considered for the tunnel, the end-restraints, the cables and the ground (0.05, 0.05, 0.03, 0.03 respectively). From the tunnel model, linearized with respect to the static equilibrium configuration, 200 vibration modes have been extracted in order to apply steps 1 and 2 of the procedure. Then, before applying step 3, that is before adding viscous damping, modeling the radiation effect, the damping matrix half-bandwidth is reduced from 469 to 386 degrees of freedom, while the stiffness half-bandwidth is instead equal to 81.

5.2. The seismic loading

A set of acceleration time histories on average compatible with the EN 1998 horizontal and vertical response spectra for a soil type C were generated with the procedure described in Section 4 and the parameters listed in Table 1. With reference to Eq. (5), the shear waves velocity is set equal to vs = 2500 ms-1 and two values of the incoherence factor, taken as $\alpha = 0.20$ and $\alpha = 0.65$, are considered. With reference to Eq. (7), t_0 was chosen as 12.5% of the generated length of the signal (20 s), t_n as $t_0 + t_{\max}$, where $t_{\max} = 10$ s. The time step is equal to 0.01s.

The acceleration time histories were generated along the tunnel at 0, 30, 50, 70, 100m, the positions of the anchorage points. The seismic motion propagates along the longitudinal direction of the tunnel, while its variability in the direction transverse to the tunnel is neglected. From the accelerations, velocity and displacement time histories are computed by integration assuming zero average velocity and zero initial displacement.

For each value of the incoherence factor, twenty realizations of the ground motion (ten for the horizontal direction and ten for the vertical direction) were generated and handled in order to obtain 20 load cases for the tunnel model. The single (three-dimensional) load case is then created selecting two different realizations for the motion in the horizontal plane, and one for the vertical direction. Furthermore, the variability of the direction of seismic motion maximum intensity has been taken into account by reducing the PGA of one of the horizontal realizations to 85% of the design PGA (0.35g), which, for testing this new kind of structure, is higher than the PGA expected at the site [14]. Finally, the water motion due to seismic waves propagation is neglected.

5.3. Results

The results of the 20+20 aforementioned non-linear dynamic analyses have been processed in order to evaluate from a statistical point of view the structural response of the tunnel; meaning that, for each response parameter, mean value, standard deviation and extreme values envelopes of the corresponding time histories have been extracted [6]. Fig. 3 depicts the envelopes of the extreme values of the bending moment in the tunnel about the horizontal axis *x*. Here, in static conditions, a negative (hogging) moment occurs along the tunnel.

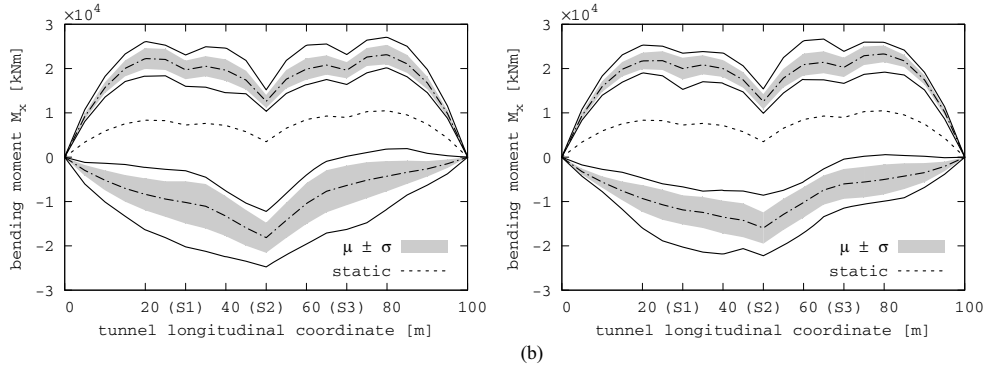

Fig. 3. Envelopes of extreme values of positive and negative tunnel bending moments about horizontal axis *x*. (a) incoherence factor $\alpha = 0.2$; (b) $\alpha = 0.625$. Static values (dashed), mean values (dash dot), minimum and maximum envelopes (solid), mean ± standard deviation interval (filled)

The shape of the bending moment distribution reflects the geometry of the adopted cable configuration since the non-linear behavior of the cables restraining the central section provides a flexible elastic bilateral/almost unilateral restraint for the horizontal/vertical motion respectively. The cables geometry and non-linear behavior couple the horizontal and vertical motion of the tunnel at this section which, under a horizontal motion, is also subject to a downward vertical displacement. This is induced by the net unbalanced vertical component of the tension in the un-slacking and slacking cables. The vertical cables do not induce a similar downward displacement. This down-pulling mechanism and the buoyancy of the tunnel are responsible for the high negative (hogging) values of bending moments and for the reduction of the maximum positive (sagging) bending moment at the central section (Fig. 3).

Moreover, the envelope of positive bending moment is distributed more evenly, since the tunnel is more effectively restrained in the upward direction and behaves, under the inertia and buoyancy forces, like a four spans beam on elastic supports. The effect of a larger value of α is to increase the asymmetry of the results. Median values slightly decrease in modulus.

6. Conclusions

This work presents the modeling and multi-support seismic analysis of Qiandao lake SFT. To perform it, a pre-existing step by step nonlinear dynamic procedure was enhanced by enriching the cable element that is used to model the mooring system, adding hydrodynamic loads. Care is given in modeling dissipation: non-linear forces model hydrodynamic effects, while radiation damping is modeled as viscous. Structural damping is accounted for accurately by enhancing a pre-existing procedure. The seismic input is defined according to a novel method that harmonizes a PSD-based RS_a spectrum with EN1998 prescriptions.

Acknowledgements

The fruitful discussions with Prof. F. Perotti, of Politecnico di Milano and the financial supports from the "Ponte di Archimede" Company and from the University of Brescia are gratefully acknowledged.

References

[1] Eurocode 8. *Design of structures for earthquake resistance, Part 1: General rules, seismic actions and rules for buildings*. EN 1998-1, 2005.

[2] Desai YM, Popplewell N, Shah A, Buragohain DN. Geometric nonlinear analysis of cable supported structures. *Computer & Structures* 1988; 29(6): 1001–9.

[3] Martinelli L, Perotti F. Numerical analysis of the non-linear dynamic behaviour of suspended cables under turbulent wind excitation. *International Journal of Structural Stability and Dynamics* 2001; 1: 207–33.

[4] Chakrabarti SK. *Hydrodynamics of Offshore Structures*. Computational Mechanics Publications-Springer-Verlag; 1987.

[5] Barbella G, Di Pilato M, Feriani A. Effects of the anchoring systems on the dynamic behaviour of the submerged floating structures (SFT). In: *AIMETA 2007, XVIII Congresso AIMETA di Meccanica Teorica e Applicata,* Brescia, Starrylink, 2007; 12.

[6] Martinelli L, Barbella G, Feriani A. Multi-support seismic input and response of submerged floating tunnels anchored by cables. *Technical Report N.6/2010*, D.I.C.A.T.A., Università degli Studi di Brescia; 2010.

[7] Feriani A, Perotti F. The formation of viscous damping matrices for the dynamic analysis of M.D.O.F. systems. *Earthquake Engineering & Structural Dynamics* 1996; 25: 689-709.

[8] Roesset JM, Whitman RV, Dobry R. Modal analysis for structures with foundation interaction. *ASCE Journal of Structural Division* 1973; 99: 399-415.

[9] Fogazzi P, Perotti F. The dynamic response of seabed anchored floating tunnels under seismic excitation. *Earthquake Engineering & Structural Dynamics* 2000; 29: 273-95.

[10] Monti G, Nuti C, Pinto PE. Nonlinear response of bridges under multisupport excitation. *Journal Of Structural Engineering* 1996; 1147-59.

[11] Shinozuka M. Monte carlo solution of structural dynamics. *Computer & Structures* 1972; 2: 855-74.

[12] Luco JE, Wong HL. Response of a rigid foundation to a spatially random ground motion. *Earthquake Engineering & Structural Dynamics* 1986; 14: 891-908.

[13] Clough RW, Penzien J. *Dynamics of Structures.* New York: McGraw-Hill; 1975.

[14] Mazzolani FM, Landolfo R, Faggiano B, Esposito M, Perotti F, Barbella G. Structural analyses of the submerged floating tunnel prototype in Qiandao Lake (PR of China). *Advances in structural Engineering* 2008; 11(4): 439-54.

[15] Sieffert JG, Cevaer F. *Handbook of Impedance Functions – Surface Foundations*. Ouest Editions, Presses Academiques; 1992.